Functional *Ex Vivo* Assay to Select Homologous Recombination–Deficient Breast Tumors for PARP Inhibitor Treatment

Kishan A.T. Naipal[1], Nicole S. Verkaik[1], Najim Ameziane[2], Carolien H.M. van Deurzen[3], Petra ter Brugge[4], Matty Meijers[5], Anieta M. Sieuwerts[6], John W. Martens[6], Mark J. O'Connor[7], Harry Vrieling[5], Jan H.J. Hoeijmakers[1], Jos Jonkers[4], Roland Kanaar[1,8,9], Johan P. de Winter[2†], Maaike P. Vreeswijk[5,10], Agnes Jager[6], and Dik C. van Gent[1]

Abstract

Purpose: Poly(ADP-ribose) polymerase (PARP) inhibitors are promising targeted treatment options for hereditary breast tumors with a homologous recombination (HR) deficiency caused by *BRCA1* or *BRCA2* mutations. However, the functional consequence of *BRCA* gene mutations is not always known and tumors can be HR deficient for other reasons than *BRCA* gene mutations. Therefore, we aimed to develop a functional test to determine HR activity in tumor samples to facilitate selection of patients eligible for PARP inhibitor treatment.

Experimental design: We obtained 54 fresh primary breast tumor samples from patients undergoing surgery. We determined their HR capacity by studying the formation of ionizing radiation induced foci (IRIF) of the HR protein RAD51 after *ex vivo* irradiation of these organotypic breast tumor samples. Tumors showing impaired RAD51 IRIF formation were subjected to genetic and epigenetic analysis.

Results: Five of 45 primary breast tumors with sufficient numbers of proliferating tumor cells were RAD51 IRIF formation deficient (11%, 95% CI, 5%–24%). This HR defect was significantly associated with triple-negative breast cancer (OR, 57; 95% CI, 3.9–825; $P = 0.003$). Two of five HR-deficient tumors were not caused by mutations in the *BRCA* genes, but by *BRCA1* promoter hypermethylation.

Conclusion: The functional RAD51 IRIF assay faithfully identifies HR-deficient tumors and has clear advantages over gene sequencing. It is a relatively easy assay that can be performed on biopsy material, making it a powerful tool to select patients with an HR-deficient cancer for PARP inhibitor treatment in the clinic. *Clin Cancer Res; 20(18); 4816–26. ©2014 AACR.*

[1]Department of Genetics, Erasmus University Medical Center, Rotterdam, the Netherlands. [2]Department of Clinical Genetics, VU University Medical Center, Amsterdam, the Netherlands. [3]Department of Pathology, Erasmus University Medical Center, Rotterdam, the Netherlands. [4]Division of Molecular Pathology, Netherlands Cancer Institute, Amsterdam, the Netherlands. [5]Department of Toxicogenetics, Leiden University Medical Center, Leiden, the Netherlands. [6]Department of Medical Oncology, Erasmus University Medical Center, Rotterdam, the Netherlands. [7]AstraZeneca, iMed Oncology, Macclesfield, Cheshire, United Kingdom. [8]Cancer Genomics Center Netherlands, Erasmus University Medical Center, Rotterdam, the Netherlands. [9]Department of Radiation Oncology, Erasmus University Medical Center, Rotterdam, the Netherlands. [10]Department of Human Genetics, Leiden University Medical Center, Leiden, the Netherlands.

Introduction

Breast cancer is the most common female cancer and the leading cause of cancer-related deaths in women (1). Great improvements have been made in breast cancer treatment with targeted therapies in estrogen receptor (ER)–positive and human epidermal growth factor receptor 2 (HER2)–positive tumors for adjuvant settings as well as treatment of metastatic breast cancer (2, 3). However, triple-negative breast cancers (TNBC), which do not express ER, progesterone receptor (PR), or HER2, have a relatively poor prognosis because of the absence of an effective targeted treatment regimen.

A particular type of TNBCs arises in familial cases of breast cancer, especially *BRCA1* mutation carriers. *BRCA1* mutation–associated tumors are predominantly high-grade TNBC (4). Interestingly, TNBCs arising in *BRCA1* mutation carriers and sporadic TNBCs share clinicopathologic and molecular characteristics. Therefore, similar etiology is proposed for these groups of breast cancer (5–7). Hereditary breast cancer associated with *BRCA1* or *BRCA2* mutations

American Association for Cancer Research

Translational Relevance

This functional assay will facilitate selection of patients with (breast) cancer for poly(ADP-ribose) polymerase (PARP) inhibitor treatment. As this is a functional test, not only known *BRCA1* and *BRCA2* mutation carriers will be identified, but also tumors with defects in other genes of the same genetic pathway and epigenetic forms of gene silencing. The assay can be performed on biopsy material, making it a powerful tool to select additional patients for ongoing and future clinical trials with PARP inhibitors. In addition to this relatively short-term translational achievement, the assay will in the long run be useful to select patients for PARP inhibitor treatment in general oncology practice for breast cancer, as well as other tumor types. We expect that the number of patients that benefit from this promising targeted cancer therapy can be increased significantly by implementing the RAD51 ionizing radiation induced foci assay.

show defects in the DNA damage response (DDR), which encompasses DNA damage repair, cell-cycle checkpoint signaling and apoptosis. *BRCA1* or *BRCA2* deficiency results in impaired double-strand break (DSB) repair by homologous recombination (HR) and chromosomal instability, which may contribute to carcinogenesis.

Dysregulation of DDR processes is a common phenomenon in cancers, sometimes highly associated with a specific type or subtype of cancer, for example, mismatch repair defects in colon carcinoma, cancer associated with crosslink repair defects in Fanconi anemia (FA), and HR defects in hereditary breast cancer (8). Interestingly, DDR defects are not only important to understand the carcinogenic process, but may also be utilized to optimize therapy response. A defective DDR pathway in tumor cells can cause dependency on another specific back up mechanism that allows cellular survival. This provides options for therapeutic intervention: specific targeting of this back up system can result in selective tumor cell death, a phenomenon referred to as "synthetic lethality" (9, 10). The major advantage of this approach is efficient tumor-specific cell killing with fewer adverse effects for the patient, because normal cells do not depend exclusively on the targeted pathway and therefore will survive the treatment. An exciting example of such a synthetic lethal approach is treatment of BRCA-deficient tumors with poly(ADP-ribose) polymerase (PARP) inhibitors (11–13).

PARP activity contributes toward signaling the presence of single-strand DNA breaks and base damage by attaching poly(ADP)ribose moieties to histones and other proteins, including itself, at the site of damage, which results in efficient repair of these types of DNA damage (14). Inhibiting PARP activity in proliferating cells results in excessive single strand and/or base lesions, which cause the collapse of replication forks and DSBs if encountered by the replication machinery (15, 16). Repair of these stalled replica-

tion fork-induced DSBs specifically requires HR (17, 18). If left unrepaired these types of lesions accumulate and cause cell death (17, 18). Therefore, HR-deficient cells associated with *BRCA1* or *BRCA2* mutations are extremely sensitive to PARP inhibition (8, 11, 12).

PARP inhibitor treatment showed a very effective antitumor activity in patients with *BRCA* mutation–associated cancers in phase I and II clinical trials (13, 19–21). Furthermore, the toxic side-effects commonly associated with conventional chemotherapy were relatively mild after PARP inhibitor treatment. Several non-*BRCA* mutation–associated tumor cell lines are also sensitive to this specific type of treatment, thereby extending the potential clinical application of PARP inhibitors. These cells had defects in genes, which also lead to impaired HR and/or cell-cycle checkpoints (22–26). These defects are also detected in human breast cancers (27). Unfortunately, in spite of promising experimental and clinical data, PARP inhibitors have not yet made it to breast cancer treatment in the clinic. One likely explanation for this is the lack of a marker for patient selection (except for known *BRCA* mutation status), because targeted treatment with PARP inhibitors can only be successful in a well-defined patient population and therefore selection of the appropriate patient population before treatment is very important.

HR activity in a tumor cell is probably the most important factor to predict whether treatment with PARP inhibitors will be successful (28). HR is mediated by the RAD51 protein that forms a nucleoprotein filament that is able to carry out the crucial strand exchange step of HR. The BRCA2 protein delivers RAD51 to DNA DSBs, where it can be detected as foci in the nucleus. Formation of RAD51 ionizing radiation induced foci (IRIF) can therefore be used as a convenient and highly informative test for HR function. Cells deficient in *BRCA1*, *BRCA2*, or a number of other HR factors do not or inefficiently form RAD51 IRIF, suggesting that this read out can be used as a PARP inhibitor sensitivity marker (28, 29). Here, we describe how *ex vivo* RAD51 IRIF formation capacity in primary breast tumor specimens can identify HR-deficient tumors.

Materials and Methods

Patient-derived xenografts

Xenograft models were initiated by implanting fresh patient-derived tumor tissue subcutaneously in the thigh of immunocompromised mice. Tumors were allowed to grow out up to 2 cm in diameter and were subsequently isolated for further experiments. To maintain the specific model *in vivo*, tumors were isolated from mice, sliced into smaller sections, and implanted in other immunocompromised mice. *BRCA1* and *BRCA2* status in tumors was analyzed by immunoblotting and exon sequencing (P. ter Brugge and J. Jonkers; unpublished data).

Clinical breast cancer specimens

Fresh breast tumor tissue was obtained from patients undergoing wide local excision or amputation for breast

cancer at Erasmus Medical Center (Erasmus MC), Haven-ziekenhuis Rotterdam, and Leiden University Medical Center (LUMC) Leiden, The Netherlands. After resection, the tissue was directly transported to the Pathology department. After macroscopic investigation and determination of tumor areas for diagnostic purposes by a pathologist, left over tumor tissue was used for research purposes according to the code of proper secondary use of human tissue in the Netherlands established by the Dutch Federation of Medical Scientific Societies and approved by the local Medical Ethical committees. Specimens were coded anonymously in a way that they were not traceable back to the patient by laboratory workers. Patients receiving neo-adjuvant chemo- or radiotherapy were excluded.

Tissue culture system

Research samples were obtained within 4 hours after surgical resection and kept at 4°C during transport to the laboratory in breast medium (30) containing a 2:1 mixture of Dulbecco's modified Eagle's medium (DMEM) without phenol red and nutrient mixture F-12 (HAM) supplemented with 2% fetal bovine serum (FBS), hydrocortisone (0.3 μg/mL; Sigma), insulin (4 μg/mL; Sigma), transferrin (4 μg/mL; Sigma), 3,3′,5-triiodothyronine (1 ng/mL; Sigma), cholera toxin (7 ng/mL; Sigma), epidermal growth factor (8 ng/mL; Sigma), adenine (0.2 mg/mL; Sigma). Excess fat tissue was discarded using surgical tools and tumor specimens were depending on tissue quantity and type of experiment, sliced into 300-μm slices using a Leica vibratome 1200S or sliced manually into approximately 2-mm slices. No differences in visualization of RAD51 IRIF were observed between these slicing methods (data not shown). Slices were directly incubated in breast medium and irradiated with 5 Gy γ-radiation using a ^{137}Cs source (0.7 Gy/min). Incubation and irradiation of samples was performed within 6 hours after surgical resection. Subsequently, samples were incubated at 37°C and 5% CO_2 on a rotating platform (60 rpm) for 2 hours. Afterward, they were fixed in 37% neutrally buffered formalin for at least 24 hours at room temperature and subsequently embedded in paraffin (overnight procedure). Microscopy sections of 4 μm were generated and subjected to immunofluorescent staining (Supplementary Fig. S1).

Immunofluorescent staining

Sections were deparaffinized using xylene and hydrated with declining concentrations of ethanol. Target antigen retrieval was performed using DAKO Antigen Retrieval buffer (pH 9.0 for RAD51 and pH 6.9 for others), which was heated to 100°C for 15 minutes. Cells were permeabilized using phosphate buffered saline (PBS) with 0.2% Triton X-100 for 20 minutes. For RAD51–geminin costaining, an additional DNase (1,000 U/mL; Roche Diagnostics) incubation was performed at 37°C for 1 hour. Blocking was achieved using PBS with 2% FBS and 1% bovine serum albumin (BSA). Primary antibodies [anti-RAD51 (GeneTex clone14B4 GTX70230) 1/200, anti-geminin (Proteintech Group 10802-1-AP) 1/400, anti-cleaved cas-

pase-3 (Cell Signaling Technology 9664S) 1/100], anti-γH2AX (Millipore 2310355) 1/500, anti-53BP1 (Novus Biologicals NB100-304) 1/500, anti-P63 (Ventana clone 4A4 790-4509, ready to use)] were diluted in blocking buffer and incubated for 90 minutes at room temperature. Secondary Alexa Fluor 594 or 488 antibodies were used to visualize the primary antibody. Sections were mounted using Vectashield mounting medium with DAPI. For P63 staining, the primary antibodies were detected using DAB chromogen.

Scoring of RAD51 foci

Tumor cells/areas were determined by morphology on a serial hematoxylin and eosin (H&E) stained section of the same tumor slice that was used for RAD51 foci analysis. Geminin-positive cells were counted manually. A cell was considered positive for geminin if the complete nucleus was stained by the geminin antibody. These cells were scored for the presence of RAD51 foci. A cell was considered positive for RAD51 foci if more than 5 nuclear foci were detected. The percentages of RAD51 foci–positive cells in the geminin-positive population were calculated. Approximately 100 geminin-positive cells were counted, unless sections had fewer geminin-positive cells, in which case at least 30 cells were counted in each tumor sample. To generate error bars, the standard error was estimated assuming a binomial distribution.

Statistical analysis

Statistical analysis were all 2-sided and performed using IBM SPSS statistics v21.

Next-generation sequencing

Genomic DNA was isolated from fresh-frozen samples of tumors using the Nucleospin Tissue Kit (Macherey-Nagel) according to the manufacturer's protocol. The percentage of tumor cells was determined by H&E staining of 5-μm cryosections of the same sample. A custom Haloplex (Agilent) Kit was used to enrich the coding regions of specific genes using 200 ng of genomic DNA to obtain sequencing libraries. Samples were tagged with a unique barcode and pooled before pair-ended sequencing 150 bp on the Illumina Miseq platform. SureCall software (Agilent) was used to detect variants. Validation of the identified mutations was performed by Sanger sequencing.

BRCA1 promoter methylation and copy number variation analysis by MS-MLPA

To assess promoter methylation of *BRCA1*, 2 MS-MLPA Kits (MRC-Holland) were used, each containing a different probe (31). Twenty-five nanograms of DNA was denatured for 10 minutes at 98°C and subsequently cooled down to 25°C. After addition of SALSA Probe-mix and MLPA buffer samples were incubated for 1 minute at 95°C followed by hybridization for 16 hours at 60°C. Next, samples were split and ligated with (methylation test) or without (copy number test) the addition of *Hha*I enzyme for 30 minutes at 49°C and then heated for 5 minutes at 98°C.

SALSA PCR-buffer and polymerase mix (including dNTPs, SALSA polymerase, and PCR primers) were added and samples were subjected to the following PCR reaction for 35 cycles: 30 seconds at 95°C; 30 seconds at 60°C; 60 seconds at 72°C. Finally, the PCR reaction was incubated at 72°C for 20 minutes. The amplified PCR products were separated by electrophoresis on an ABI PRISM 310 fragment analyzer (Applied Biosystems) and analyzed using Gene-marker analysis software (Softgenetics).

In situ detection of BRCA1 RNA

In situ detection of BRCA1 mRNA was performed using RNAScope (ACD) using standard protocols as described by the manufacturer (32). BRCA1 probes were purchased from the same company. In short, paraffin sections were depar-affinized with xylene and samples were subjected to pre-treatment steps described by the manufacturer. Next, hybridization of target probes [BRCA1 along with POLR2A (positive control) and DapB (negative control)] was achieved by incubating samples with specific probes for 2 hours at 40°C. Subsequently, several amplification steps were performed using specific amplification buffers to amplify the hybridized probe signal and visualization of this signal was achieved using Fast Red dye. Samples were counterstained with Mayer's hematoxylin solution and mounted using EcoMount mounting medium.

Results

Ex vivo RAD51 IRIF formation in xenograft tumors

Cells in the S or G_2 phase of the cell cycle form RAD51 foci after DSB induction by IR. We adapted the immunofluo-rescence detection of these IRIF for thin breast tumor tissue slices and investigated whether we could distinguish tumors with known defects in BRCA1 or BRCA2 from other tumors by analyzing RAD51 IRIF formation. To validate our pro-cedures, we used a collection of BRCA-positive and -nega-tive human to mouse xenograft tumor models. Conditions for culturing tissue slices derived from these xenograft tumors were optimized (Naipal and colleagues, in prepa-ration), slices were irradiated ex vivo, fixed after 2 hours and RAD51 IRIF formation was analyzed (Supplementary Fig. S1). The 2-hour time point was optimal for RAD51 IRIF formation (ref. 33 and Supplementary Fig. S2A). As RAD51 IRIF are only expected to occur in S- or G_2-phase cells, we also identified this cell population in the tumor slices by staining for the cell-cycle marker geminin (refs. 34 and 35; Fig. 1A). Indeed, RAD51 IRIF–positive nuclei were only found in irradiated geminin-positive cells (ref. 35 and Supplementary Fig. S2B).

In a blinded experimental setup we found all tumors without a known DDR defect ($n = 4$) to display prominent RAD51 IRIF in more than 50% of geminin-positive cells (Fig. 1B). On the other hand, we observed less than 10% of geminin-positive cells exhibited RAD51 IRIF in organotypic slices from tumors with known BRCA1 or BRCA2 ($n = 8$) defects. BRCA1 deficiency caused by a frame shift mutation or a BRCA1 promoter hypermethylation both displayed

absence of RAD51 foci in xenograft tumors, showing that genetic and epigenetic modes of gene inactivation have similar RAD51 foci–deficient phenotypes in this assay. In cells without geminin expression, we did not detect RAD51 IRIF and tumors proficient for BRCA1 or BRCA2 that were not irradiated formed RAD51 foci in less than 10% of geminin-positive cells (Fig. 1A and B), showing that the assay is specific for induction of foci by IR in S- and G_2-phase cells.

Ex vivo RAD51 IRIF formation in human breast tumors

We investigated whether this assay could also be used for clinical tumor specimens with a known BRCA1 defect. We obtained a tumor biopsy from a patient carrying a germline BRCA1 mutation who had developed a retrosternal recur-rence after previous primary breast cancer treatment. In this tumor, only 11% of geminin-positive cells displayed RAD51 IRIF, whereas tumor slices from unselected primary tumors ($n = 5$) showed RAD51 IRIF in more than 50% of the geminin-positive cells (Fig. 2A and B). Results from the xenografts and the patient biopsy indicate that RAD51 IRIF can be identified in ex vivo irradiated organotypic tumor slices and that this assay can be used to discriminate HR-deficient and HR-proficient tumors.

After validation, we used this assay to identify HR defects in clinical breast cancer specimens. We collected 54 (che-motherapy naïve) tumor samples obtained from patients that underwent breast cancer surgery and generated orga-notypic tumor slices. Information about BRCA mutation status, family history, and pathology reports were unknown to the investigators during the analysis of the tumor sam-ples. Pathology reports from corresponding tumors were obtained afterward (Supplementary Table S1). The majority of tumors were histologically classified as ductal carcinoma (82%; $n = 44$) whereas 15% ($n = 8$) was classified as lobular carcinoma. In addition, 93% ($n = 50$) of the samples expressed either ER, PR, or HER2 receptor and 7% ($n = 4$) of tumors had no expression of these 3 receptors (TNBC) as determined by immunohistochemical analysis. Nine tumor samples contained very low numbers of geminin-expressing cells and could therefore not be analyzed. There was no specific correlation between low geminin expression and pathologic tumor characteristics (Supplementary Table S2), suggesting that this was the result of coincidental sampling of tumor areas that were less proliferative or exhibited rapid decrease in proliferation after resection. In total, 45 tumor samples contained sufficient numbers of geminin-positive cells for RAD51 IRIF analysis.

Clinicopathologic characteristics of RAD51 IRIF–negative tumors

Based on results of xenograft experiments, RAD51 IRIF formation was considered normal (positive) when more than 5 foci per nucleus were present in more than 50% of geminin-positive cells, whereas RAD51 IRIF formation was considered impaired (negative) when less than 20% of geminin-expressing cells contained more than 5 RAD51 IRIF per cell. Using these criteria, 5 tumors of 45 (11%;
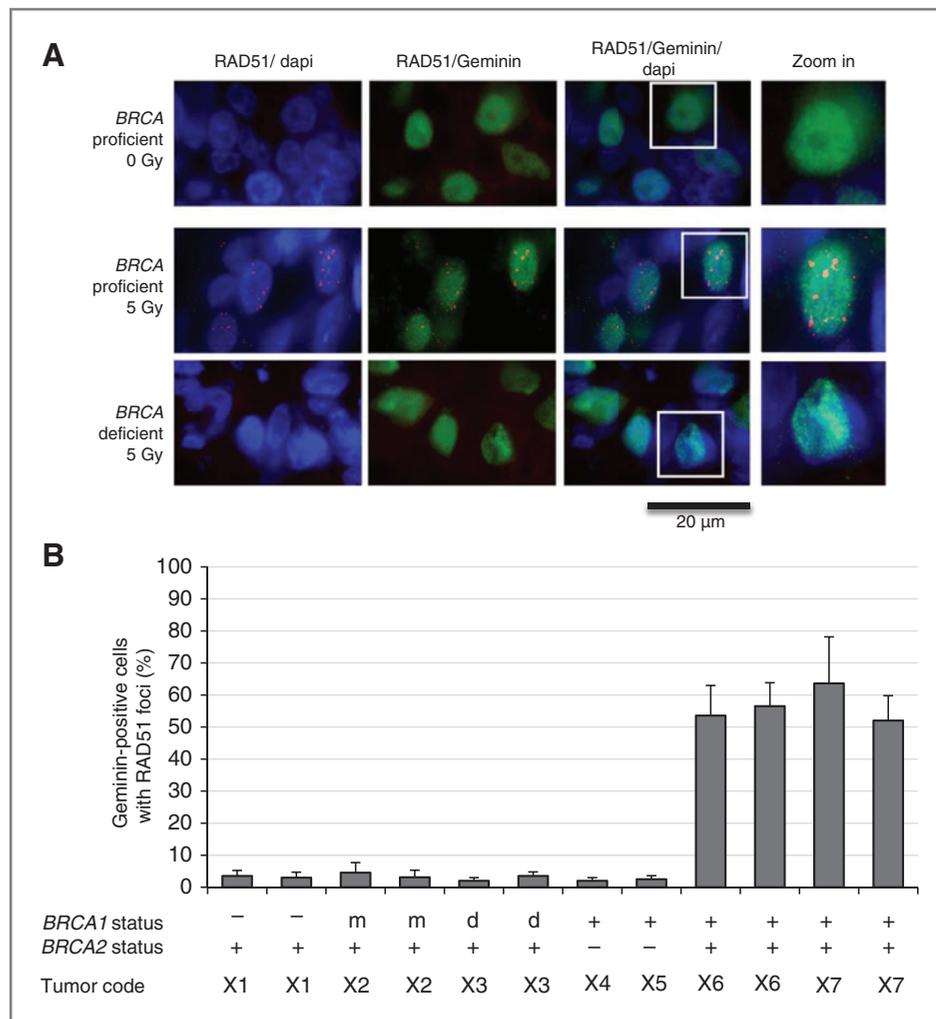
Figure 1. RAD51 IRIF in xenograft breast tumors. A, representative pictures of tumor cells in slices of *BRCA*-deficient and *BRCA*-proficient xenograft tumors. RAD51 IRIF are present in the majority of geminin-positive cells in *BRCA*-proficient tumors but not in *BRCA*-deficient tumors. Tumor samples were subjected to 5 Gy γ radiation, cultured at 37°C and fixed 2 hours after irradiation. Right column of images represent single-cell enlargements of cells in white boxes; blue, DAPI; green, geminin; and red, RAD51; scale bar, 20 μm. B, quantification of RAD51 IRIF in xenograft tumor samples. At least 30 geminin-positive cells were counted for each sample. −, gene inactivation caused by *BRCA1* mutation; m, gene inactivation caused by *BRCA1* promoter hypermethylation; d, no mutation in *BRCA1* but absent BRCA1 expression on immunoblot. Cause unknown. Same tumor codes represent duplicate analysis of the same xenograft tumor but in different mice at different times. Error bars indicate standard error assuming binomial distribution.

95% CI, 5%–24%) showed impaired RAD51 IRIF formation (Fig. 3). We excluded technical reasons for the absence of RAD51 foci in tumor cells by showing formation of γH2AX and 53BP1 nuclear foci after irradiation (Supplementary Fig. S3A). Furthermore, normal RAD51 IRIF formation was detected in geminin-positive normal breast epithelium, stroma or fat tissue within the same tissue section (Supplementary Fig. S4). Lobular carcinomas in this cohort did not show impaired RAD51 IRIF (0 of 7), whereas tumors from the histologic subtypes classified as ductal carcinoma (3 of 35) or other (not classified ductal or lobular, 2 of 2) had impaired focus formation (Table 1). In addition, RAD51 IRIF–negative tumors were frequently classified as grade 3 carcinomas, although this correlation was not statistically significant ($P = 0.419$; Table 1). Three of 5 RAD51 IRIF–negative tumors were TNBC whereas the 2 other tumors expressed the ER (Table 1). Interestingly, 3 of 4 TNBC tumors in this cohort displayed impaired RAD51 IRIF formation, indicating that HR defects were more frequent in TNBC than receptor-positive BC (OR, 57; 95% CI, 3.9–825.4; $P = 0.003$; Table 1).

One of the 45 tumors (sample #30) in the cohort displayed great variability in RAD51 IRIF formation. RAD51 IRIF–positive cells (>5 foci/cell) were clearly recognized, but lower in number compared with other tumors. Strikingly, in some regions of the tumor RAD51 IRIF–positive cells were completely absent although geminin-positive cells were present in high numbers, similar to that of other tumors (data not shown). Overall RAD51 IRIF were observed in 38% of geminin-positive cells (Fig. 3). Notably, this tumor sample was derived from a 102-year-old patient (Supplementary Table S1); the oldest patient in this cohort. All other tumors showed little variability in RAD51 IRIF formation, indicating that analysis of a small area of the tumor will in most cases be sufficient to accurately determine RAD51 IRIF formation proficiency.

Ex vivo PARP inhibitor sensitivity in RAD51 IRIF–negative tumor

One RAD51 IRIF–negative tumor (sample #20) was incubated *ex vivo* with the PARP inhibitor, Olaparib. After 96 hours treatment, this tumor sample showed a clearly

Figure 2. Validation of RAD51 IRIF in human breast tumors. A, impaired RAD51 IRIF formation in *BRCA1*-deficient breast cancer. Immunofluorescent images showing the absence of RAD51 foci in *BRCA*-mutated tumor sample in contrast to a primary tumor from another patient. Tumor samples were subjected to 5 Gy γ radiation, cultured at 37°C and fixed 2 hours after irradiation. Right column of images represent single-cell enlargements of cells in white boxes; blue, DAPI; green, geminin; and red, RAD51; scale bar, 20 μm. B, quantification of RAD51 IRIF in tumor samples displays lower formation of foci in a *BRCA* deficient tumor than in 5 unselected tumors. All tumor samples were collected shortly after each other from the clinic and stained simultaneously. At least 30 geminin-positive cells were counted for each sample. Error bars indicate standard error assuming binomial distribution.
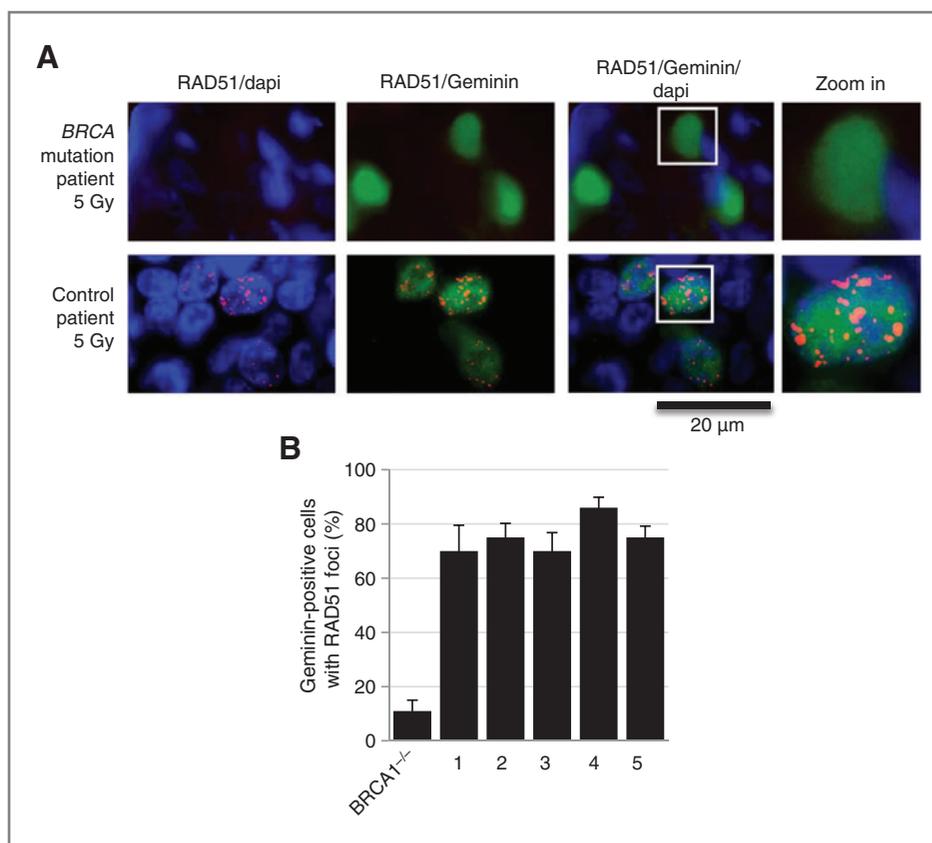
altered morphology with many picnotic nuclei, compared with the untreated tumor slice (Fig. 4A). The tumor cell nuclei in the treated sample were either larger in size or fragmented, shrunken, and hyperchromatic. Interestingly, the morphology of the normal mammary ducts (identified by their typical double layer of glandular cells and surrounding P63-positive myoepithelial cells) was not affected by Olaparib treatment (Fig. 4B). Subsequent staining of the sections showed increased levels of the apoptotic marker cleaved caspase-3 after 96 hours of exposure to Olaparib (Fig. 4C). In 5 tumors with normal formation of RAD51 IRIF, the altered morphology and induction of cleaved caspase-3 was not noticed after this treatment, strongly suggesting that induction of apoptosis was because of PARP inhibitor treatment and not caused by declining tissue viability (Fig. 4A and C).

PARP inhibition results in DSBs during replication. This was shown by the formation of γH2AX and 53BP1 nuclear foci (Supplementary Fig. S3B). As a consequence we expected an activated HR pathway and thus formation of RAD51 foci in HR-proficient cells after PARP inhibitor treatment. Accordingly, RAD51 foci induced by Olaparib treatment were present in normal mammary epithelium and not in tumor cells in the same tissue slice (Fig. 4B). These results indicate that the functional HR defect in these tumor cells caused sensitivity to PARP inhibitors, whereas normal epithelial cells were not affected, opening perspec-

tives for using this assay as a functional test for clinical sensitivity.

Genetic and epigenetic analysis of RAD51 IRIF–negative tumors

Subsequently, we determined the basis for impaired RAD51 IRIF formation in the tumors by genetic analysis for the *BRCA1* and *BRCA2* genes in these tumors. We sequenced more than 99% of the *BRCA1*, *BRCA2*, and *TP53* exons and flanking intron sequences and found that 3 RAD51 IRIF–negative tumors harbored a mutation in the *BRCA2* gene (Table 2). Two of these tumors were ER positive and one was a TNBC (Table 2). In sample #2, we identified a G to T mutation at the splice donor site of intron 15 (c.7617 + 1G > T, NM_000059) causing aberrant splicing with skipping of exon 15 as a result. This mutation was detected hemi/homozygously in the tumor, whereas normal breast tissue from the same patient was heterozygous for this mutation. This showed that the patient carried a germline mutation in the *BRCA2* gene (Supplementary Fig. S5A). Sample #54 harbored a known pathogenic missense mutation (c.9154C > T, p.Arg3052Trp, NM_000059) in the *BRCA2* gene. Interestingly, this specific sample was obtained from the only male patient in this cohort. The other *BRCA2* mutation was detected in sample #32, a TNBC (Table 2). This specific mutation (c.517G > C, p.Gly173Arg, NM_000059) at the intron–exon junction alters the first
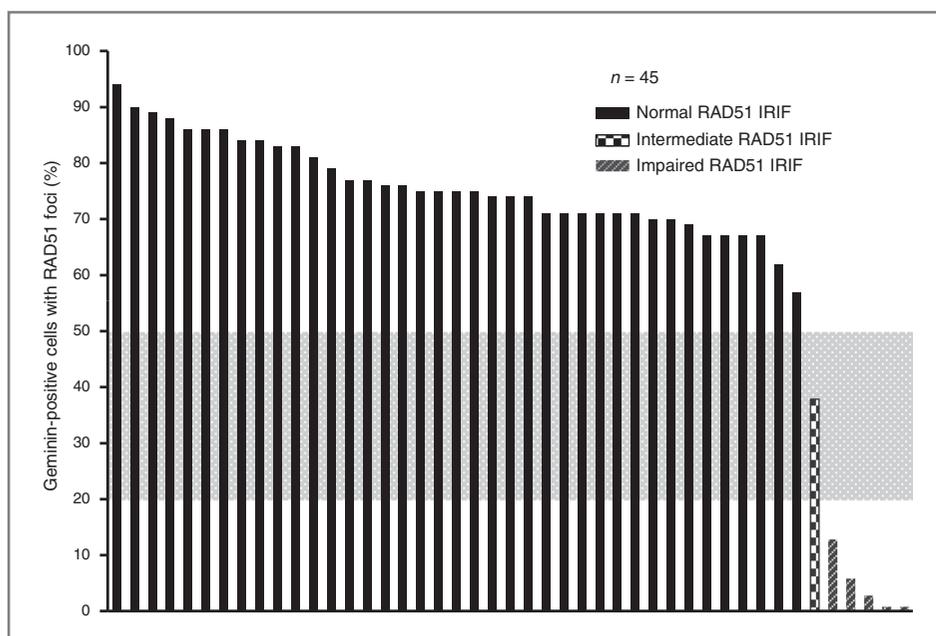
Figure 3. RAD51 IRIF in 45 primary breast tumor samples. Impaired RAD51 IRIF formation was detected in 5 of 45 primary breast tumor samples. Each bar represents the quantification of RAD51 IRIF in a tumor sample. At least 30 geminin-positive cells per tumor were counted. A cell was considered positive for RAD51 IRIF if more than 5 foci were present in the nucleus. Normal RAD51 IRIF >50%, intermediate RAD51 IRIF = 20% to 50%, impaired RAD51 IRIF <20%.

nucleotide of exon 7, which might abrogate splicing of exon 7. Gene sequencing of the 2 remaining tumors (sample #1 and #20), both TNBC, did not reveal mutations in the *BRCA1* and *BRCA2* genes but did reveal a mutation in *TP53*, which is very often detected in TNBC (ref. 36; Table 2).

BRCA1 promoter hypermethylation can lead to reduced BRCA1 protein expression and lack of RAD51 IRIF forma-tion (ref. 37 and Fig. 1). Therefore, we analyzed hyper-methylation of the *BRCA1* promoter in the RAD51 IRIF–negative tumors. Sample #1 and #20, both displayed hyper-methylation in the promoter sequence of the *BRCA1* gene (Table 2 and Supplementary Fig. S5B). This was not observed in normal mammary tissue from the same patients, suggesting that impaired RAD51 IRIF formation

Table 1. Clinicopathologic comparison of normal RAD51 IRIF versus impaired RAD51IRIF tumor samples

$n = 44$	Normal RAD51 IRIF $n = 39$	Impaired RAD51 IRIF $n = 5$	P
Histologic subtype			
Ductal carcinoma	32 (82%)	3 (60%)	
Lobular carcinoma	7 (18%)	0 (0%)	
Other	0 (0%)	2 (40%)	0.014[a]
Histologic grade			
1	6 (15%)	0 (0%)	
2	16 (41%)	1 (20%)	
3	17 (44%)	4 (80%)	0.419
Receptor status			
ER/PR$^+$	35 (90%)	2 (40%)	
ER/PR$^-$	4 (10%)	3 (60%)	0.023[a]
HER2$^+$	5 (13%)	0 (0%)	
HER2$^-$	34 (87%)	5 (100%)	1.000
TN	1 (3%)	3 (60%)	
ER/PR/HER2$^+$	38 (97%)	2 (40%)	0.003[a]
Tumor size (ø cm) (median–range)	2.7–11.7	4.8–4.4	0.767
Age (y) at surgery (median–range)	63–56	74–16	0.405

NOTE: For categorical data, the P values were calculated using the Fisher exact test and for continuous data (age and tumor size) P values were calculated using the Mann–Whitney test. One intermediate RAD51 IRIF tumor is not represented in this table.
[a]Statistically significant differences (P < 0.05).

Figure 4. *Ex vivo* sensitivity for olaparib in RAD51 IRIF–negative tumor. Cytotoxic response of a RAD51 IRIF–negative tumor to PARP inhibitor treatment *ex vivo*. A, tumor sample #20 with impaired RAD51 IRIF formation displays altered morphology and picnotic nuclei after a 96-hour incubation with 10 μmol/L olaparib compared with a breast tumor with normal RAD51 IRIF formation. B, different regions from the same tumor slice (#20) incubated with 10 μmol/L olaparib for 96 hours. Normal mammary epithelium, supported by P63 staining, displays normal nuclear morphology. Also, formation of RAD51 foci is normal in these cells, whereas tumor cells do not form RAD51 foci. Right column of images represent single-cell enlargements of cells in white boxes; brown, P63; blue, DAPI; green, geminin; and red, RAD51. C, tumor cells display high expression of the apoptotic marker, cleaved caspase-3, in response to treatment; blue, DAPI; red, cleaved caspase-3.
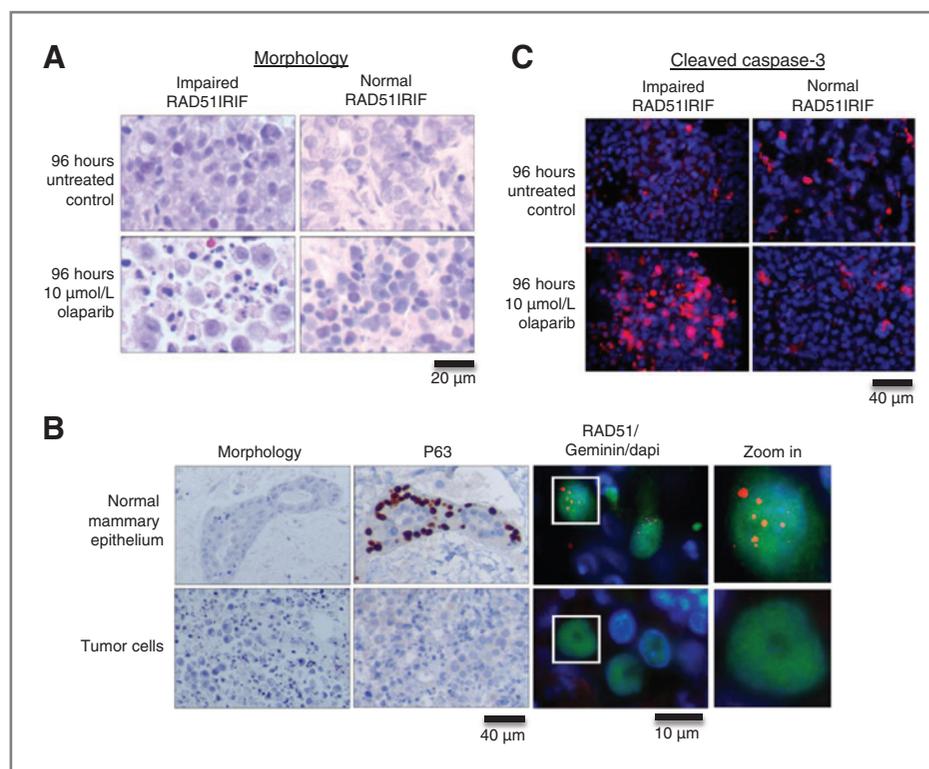
in the tumor was caused by *BRCA1* promoter hypermethylation (Supplementary Fig. S5B). *BRCA1* promoter methylation was not detected in the other 3 RAD51 IRIF–negative tumors, nor in 10 random RAD51 IRIF-positive tumors (data not shown). To assess the functionality of *BRCA1* promoter hypermethylation, we performed *in situ* detection of *BRCA1* mRNA. As expected, we did not detect *BRCA1* mRNA in sample #1 and #20, whereas *BRCA1* mRNA was readily observed in unmethylated tumors (Supplementary Fig. S6 and data not shown). This confirms that *BRCA1* promoter methylation caused *BRCA1* silencing and impaired RAD51 IRIF formation.

The remaining TNBC with normal RAD51 IRIF formation (sample #62) did not harbor a mutation in *BRCA1* or *BRCA2*, neither did it show hypermethylation of the *BRCA1* promoter (Table 2). The only sample that showed intermediate levels of RAD51 IRIF also did not harbor a mutation in *BRCA1* or *BRCA2* and showed no hypermethylation of the *BRCA1* promoter (Table 2). In conclusion, all tumors with impaired RAD51 IRIF in this cohort were found to harbor *BRCA1* or *BRCA2* defects.

Discussion

Here we describe an assay to identify HR-deficient tumors based on RAD51 IRIF formation in organotypic tumor slices *ex vivo*. The assay was validated in xenograft tumors with defective or normal *BRCA1/2* gene expression, where the

Table 2. Genetic analysis of tumor samples

Sample number	Receptor status	*BRCA1*	*BRCA2*	*TP53*	RAD51 IRIF
1	TNBC	Promoter methylation	Normal	c.581T > C	Impaired
20	TNBC	Promoter methylation	Normal	c.1024C > T	Impaired
32	TNBC	Normal	c.517G > C p.Gly173Arg	c.154C > T	Impaired
62	TNBC	Normal	Normal	c.532dup	Normal
2	ER+	Normal	c.7617 + 1G > T	Normal	Impaired
54	ER+	Normal	c.9154C > T p.Arg3052Trp	Normal	Impaired
30	ER+	Normal	Normal	c.711G > A	Intermediate

Abbreviations: ER+, estrogen receptor–positive breast cancer; normal, no mutation and no *BRCA1* promoter methylation.

absence of RAD51 IRIF perfectly correlated with *BRCA* gene status. We used this approach to identify a subgroup of HR-deficient tumors in patients with primary breast cancer and found that approximately 10% of primary breast tumors has a clearly impaired HR repair capacity based on this assay. This percentage is lower than some estimates described in other publications, which report that up to 25% of sporadic breast cancers have a BRCAness phenotype and might be related to a possible HR deficiency (38). Other research groups report even higher percentages of primary breast tumors to have impaired HR based on a RAD51 focus formation assay (35, 39, 40). There are several explanations for these discrepancies.

One explanation could be that there are differences in the methods used to induce, visualize, and characterize RAD51 foci in tumor samples. In some studies, the foci were induced by DNA damage caused by *in vivo* administration of chemotherapy to patients with breast cancer (35, 40). The foci were visualized in tumor biopsies of these patients obtained 24 hours after the first dose of chemotherapy. This method might result in an overestimation of HR-deficient tumors, because efficient DNA repair will result in relatively low levels of residual foci at 24 hours after treatment (33, 41). Therefore, a low number of residual RAD51 foci does not necessarily mean impaired focus formation. In contrast, we induced DNA damage by IR of tumor samples *ex vivo* and subsequent culturing for 2 hours before RAD51 foci were visualized. In cell culture and *ex vivo* tissue culture, the number of RAD51 foci peaks 2 hours after DNA damage treatment (33, 41). Thus, in contrast to detecting RAD51 foci 24 hours after the *in vivo* administration of chemotherapy, our assay specifically detects the ability to form RAD51 foci in the tumor samples. Moreover, after robust validation of the *ex vivo* irradiation approach, we can state with high confidence that this assay faithfully discriminates HR-deficient from HR-proficient tumors.

Another methodological difference that could lead to an overestimation of HR-deficient tumors is the fact that some research groups analyze the formation of RAD51 foci without adjusting for proliferating cells in the tumor samples. As HR is only active during the S and G_2 phases of the cell cycle, RAD51 focus formation is only expected in these cell-cycle phases. Thus, tumor samples with very few cells in the S–G_2 phases will have low levels of RAD51 foci, but these tumors are not necessarily impaired in RAD51 IRIF formation. Therefore, we only score RAD51 foci in cells expressing geminin, which is a marker for the S and G_2 phases of the cell cycle (34, 35, 42, 43). We identified some tumor samples having no or very few cells with geminin expression. This might be a result of a very low-proliferating tumor area or coincidental sampling of a part of the tumor that rapidly declined in proliferation after surgical resection. Therefore, we exclude samples with low geminin expression (less than 30 geminin-positive cells) from quantitative analysis to prevent inappropriate designation of tumors as HR deficient.

HR defects in ER-positive BC might be indicative for a *BRCA2* mutation (38). The fact that we identify *BRCA2*

mutations in the 2 HR-deficient ER-positive tumors is therefore within expectations. On the other hand, TNBC more frequently harbor a mutation in *BRCA* genes and among TNBC the incidence of *BRCA1* mutations is higher than *BRCA2* mutations (38, 44, 45). In the RAD51 IRIF-negative TNBCs, we did not identify mutations in the *BRCA1* gene, but instead found hypermethylation of the *BRCA1* promoter as a cause for the RAD51 IRIF defect. Therefore, the absence of RAD51 IRIF in the tumor could in all cases be explained by the deficiency of *BRCA1* or *BRCA2*. Thus, mutation screening of *BRCA1* and *BRCA2* in combination with methylation analysis of the *BRCA1* promoter, would have been sufficient to identify these tumors. However, other causes for HR deficiency in primary BC have been described in literature (22, 46, 47). These specific defects are probably less frequently observed in the population but are expected to be present when screening a larger cohort of primary BC by the RAD51 IRIF assay.

Nevertheless, the observed frequency of RAD51 IRIF deficiency in TNBC suggests that this subgroup of breast tumors should benefit the most from PARP inhibitor treatment. However, in a phase II clinical trial, treatment of non–BRCA-associated advanced TNBC with a daily dose of Olaparib did not result in objective responses (21). There are several possible explanations for the lack of response. The sample size was small and it is likely that not all TNBC are HR deficient. In addition, the fact that the patients included in this clinical trial had previously been treated with several cycles and types of chemotherapy, probably with DNA-damaging agents, might have caused a selection of resistant tumor cells that are also resistant to PARP inhibitors.

A possible mechanism leading to PARP inhibitor resistance in *BRCA1*-deficient cells is 53BP1 loss, which also restores RAD51 focus formation (48). Other mechanisms causing resistance to PARP inhibitors are secondary mutations in *BRCA* genes that are able to restore the open reading frame and result in transcription of functional isoforms of BRCA proteins (49). We therefore argue that the *ex vivo* assay will also be a very useful tool to discriminate tumors that acquired resistance by these mechanisms.

Currently, phase III clinical trials are being conducted for different PARP inhibitors. However, patient selection is based on germline *BRCA* mutations. Other assays to determine HR status have been proposed and certain trials take this into account, for example, Myriad's HRD assay. The advantage of this assay is that it can be performed on formalin-fixed paraffin-embedded (FFPE) material and no fresh viable tissue is needed. It measures loss of heterozygosity caused by HR deficiency in the tumor (50). This gives a historic overview of genomic aberrations acquired by the tumor over time. Although the RAD51 IRIF assay can only be performed on fresh tumor material, it provides a functional analysis of HR at the moment of sampling, that might also discriminate tumors that have acquired resistance to PARP inhibitors or other DNA damaging drugs.

Concluding, we show that functional assessment of HR in breast tumors, by *ex vivo* determination of RAD51 IRIF formation in organotypic slices, provides a unique chance

to identify a sizeable fraction of HR-deficient tumors among unselected primary breast tumors. This has a clear advantage over gene sequencing as more than only *BRCA* mutation associated tumors are identified as HR deficient. Based on the study presented here, we expect approximately 10% of all patients with breast cancer to be eligible for PARP inhibitor treatment. Furthermore, other chemotherapeutic treatments, causing DNA damage that requires HR for its repair, could also be considered for this subgroup of mammary tumors. Most notably, the interstrand crosslinking agent cis-Platin or the topoisomerase I inhibitor Doxorubicin are expected to have efficient cell killing capacity in this category of tumors. Therefore, this assay grants unique opportunities to select patients for clinical trials with PARP inhibitors and to facilitate optimal selection of current standard treatment options.

Disclosure of Potential Conflicts of Interest

No potential conflicts of interest were disclosed.

Authors' Contributions

Conception and design: K.A.T. Naipal, N.S. Verkaik, M.J. O'Connor, H. Vrieling, J.H.J. Hoeijmakers, R. Kanaar, M.P. Vreeswijk, A. Jager, D.C. van Gent
Development of methodology: K.A.T. Naipal, N.S. Verkaik, M. Meijers, H. Vrieling, M.P. Vreeswijk, A. Jager, D.C. van Gent
Acquisition of data (provided animals, acquired and managed patients, provided facilities, etc.): K.A.T. Naipal, N.S. Verkaik, C.H.M. van Deurzen, P. ter Brugge, A.M. Sieuwerts, J.W. Martens, J. Jonkers, M.P. Vreeswijk

Analysis and interpretation of data (e.g., statistical analysis, biostatistics, computational analysis): K.A.T. Naipal, N.S. Verkaik, N. Ameziane, M. Meijers, J.W. Martens, H. Vrieling, M.P. Vreeswijk, A. Jager, D.C. van Gent, J. de Winter
Writing, review, and/or revision of the manuscript: K.A.T. Naipal, N.S. Verkaik, N. Ameziane, C.H.M. van Deurzen, J.W. Martens, H. Vrieling, J.H.J. Hoeijmakers, R. Kanaar, A. Jager, D.C. van Gent, J. de Winter
Administrative, technical, or material support (i.e., reporting or organizing data, constructing databases): K.A.T. Naipal, N.S. Verkaik, N. Ameziane, M. Meijers
Study supervision: R. Kanaar, M.P. Vreeswijk, A. Jager, D.C. van Gent

References

1. Parkin DM, Bray F, Ferlay J, Pisani P. Global cancer statistics, 2002. CA Cancer J Clin 2005;55:74–108.
2. Campos SM, Winer EP. Hormonal therapy in postmenopausal women with breast cancer. Oncology 2003;64:289–99.
3. Madarnas Y, Trudeau M, Franek JA, McCready D, Pritchard KI, Messersmith H. Adjuvant/neoadjuvant trastuzumab therapy in women with HER-2/neu-overexpressing breast cancer: a systematic review. Cancer Treat Rev 2008;34:539–57.
4. Turner NC, Reis-Filho JS. Basal-like breast cancer and the BRCA1 phenotype. Oncogene 2006;25:5846–53.
5. Lips EH, Mulder L, Oonk A, van der Kolk LE, Hogervorst FB, Imholz AL, et al. Triple-negative breast cancer: BRCAness and concordance of clinical features with BRCA1-mutation carriers. Br J Cancer 2013; 108:2172–7.
6. Joosse SA, Brandwijk KI, Mulder L, Wesseling J, Hannemann J, Nederlof PM. Genomic signature of BRCA1 deficiency in sporadic basal-like breast tumors. Genes Chromosomes Cancer 2011;50: 71–81.
7. Turner NC, Reis-Filho JS, Russell AM, Springall RJ, Ryder K, Steele D, et al. BRCA1 dysfunction in sporadic basal-like breast cancer. Oncogene 2007;26:2126–32.
8. Curtin NJ. DNA repair dysregulation from cancer driver to therapeutic target. Nat Rev Cancer 2012;12:801–17.
9. Bouwman P, Jonkers J. The effects of deregulated DNA damage signalling on cancer chemotherapy response and resistance. Nat Rev Cancer 2012;12:587–98.
10. Rehman FL, Lord CJ, Ashworth A. Synthetic lethal approaches to breast cancer therapy. Nat Rev Clin Oncol 2010;7:718–24.
11. Bryant HE, Schultz N, Thomas HD, Parker KM, Flower D, Lopez E, et al. Specific killing of BRCA2-deficient tumours with inhibitors of poly (ADP-ribose) polymerase. Nature 2005;434:913–7.
12. Farmer H, McCabe N, Lord CJ, Tutt AN, Johnson DA, Richardson TB, et al. Targeting the DNA repair defect in BRCA mutant cells as a therapeutic strategy. Nature 2005;434:917–21.

13. Fong PC, Boss DS, Yap TA, Tutt A, Wu P, Mergui-Roelvink M, et al. Inhibition of poly(ADP-ribose) polymerase in tumors from BRCA mutation carriers. N Engl J Med 2009;361:123–34.
14. de Murcia G, Menissier de Murcia J. Poly(ADP-ribose) polymerase: a molecular nick-sensor. Trends Biochem Sci 1994;19:172–6.
15. Plummer ER. Inhibition of poly(ADP-ribose) polymerase in cancer. Curr Opin Pharmacol 2006;6:364–8.
16. Helleday T. The underlying mechanism for the PARP and BRCA synthetic lethality: clearing up the misunderstandings. Mol Oncol 2011;5:387–93.
17. Helleday T. Homologous recombination in cancer development, treatment and development of drug resistance. Carcinogenesis 2010;31: 955–60.
18. Petermann E, Orta ML, Issaeva N, Schultz N, Helleday T. Hydroxyurea-stalled replication forks become progressively inactivated and require two different RAD51-mediated pathways for restart and repair. Mol Cell 2010;37:492–502.
19. Tutt A, Robson M, Garber JE, Domchek SM, Audeh MW, Weitzel JN, et al. Oral poly(ADP-ribose) polymerase inhibitor olaparib in patients with BRCA1 or BRCA2 mutations and advanced breast cancer: a proof-of-concept trial. Lancet 2010;376:235–44.
20. Gelmon KA, Tischkowitz M, Mackay H, Swenerton K, Robidoux A, Tonkin K, et al. Olaparib in patients with recurrent high-grade serous or poorly differentiated ovarian carcinoma or triple-negative breast cancer: a phase 2, multicentre, open-label, non-randomised study. Lancet Oncol 2011;12:852–61.
21. Sandhu SK, Omlin A, Hylands L, Miranda S, Barber LJ, Riisnaes R, et al. Poly (ADP-ribose) polymerase (PARP) inhibitors for the treatment of advanced germline BRCA2 mutant prostate cancer. Ann Oncol 2013;24:1416–8.
22. McCabe N, Turner NC, Lord CJ, Kluzek K, Bialkowska A, Swift S, et al. Deficiency in the repair of DNA damage by homologous recombination and sensitivity to poly(ADP-ribose) polymerase inhibition. Cancer Res 2006;66:8109–15.

23. Lord CJ, McDonald S, Swift S, Turner NC, Ashworth A. A high-throughput RNA interference screen for DNA repair determinants of PARP inhibitor sensitivity. DNA Repair (Amst) 2008;7:2010–9.

24. Turner NC, Lord CJ, Iorns E, Brough R, Swift S, Elliott R, et al. A synthetic lethal siRNA screen identifying genes mediating sensitivity to a PARP inhibitor. EMBO J 2008;27:1368–77.

25. Murai J, Huang SY, Das BB, Renaud A, Zhang Y, Doroshow JH, et al. Trapping of PARP1 and PARP2 by clinical PARP inhibitors. Cancer Res 2012;72:5588–99.

26. Dedes KJ, Wilkerson PM, Wettersog D, Weigelt B, Ashworth A, Reis-Filho JS. Synthetic lethality of PARP inhibition in cancers lacking BRCA1 and BRCA2 mutations. Cell Cycle 2011;10:1192–9.

27. Cancer Genome Atlas N. Comprehensive molecular portraits of human breast tumours. Nature 2012;490:61–70.

28. Mukhopadhyay A, Elattar A, Cerbinskaite A, Wilkinson SJ, Drew Y, Kyle S, et al. Development of a functional assay for homologous recombination status in primary cultures of epithelial ovarian tumor and correlation with sensitivity to poly(ADP-ribose) polymerase inhibitors. Clin Cancer Res 2010;16:2344–51.

29. Oplustilova L, Wolanin K, Mistrik M, Korinkova G, Simkova D, Bouchal J, et al. Evaluation of candidate biomarkers to predict cancer cell sensitivity or resistance to PARP-1 inhibitor treatment. Cell Cycle 2012;11:3837–50.

30. Garvin S, Nilsson UW, Huss FR, Kratz G, Dabrosin C. Estradiol increases VEGF in human breast studied by whole-tissue culture. Cell Tissue Res 2006;325:245–51.

31. Nygren AO, Ameziane N, Duarte HM, Vijzelaar RN, Waisfisz Q, Hess CJ, et al. Methylation-specific MLPA (MS-MLPA): simultaneous detection of CpG methylation and copy number changes of up to 40 sequences. Nucleic Acids Res 2005;33:e128.

32. Wang F, Flanagan J, Su N, Wang LC, Bui S, Nielson A, et al. RNAscope: a novel in situ RNA analysis platform for formalin-fixed, paraffin-embedded tissues. J Mol Diagn 2012;14:22–9.

33. van Veelen LR, Essers J, van de Rakt MW, Odijk H, Pastink A, Zdzienicka MZ, et al. Ionizing radiation-induced foci formation of mammalian Rad51 and Rad54 depends on the Rad51 paralogs, but not on Rad52. Mutat Res 2005;574:34–49.

34. Wohlschlegel JA, Kutok JL, Weng AP, Dutta A. Expression of geminin as a marker of cell proliferation in normal tissues and malignancies. Am J Pathol 2002;161:267–73.

35. Graeser M, McCarthy A, Lord CJ, Savage K, Hills M, Salter J, et al. A marker of homologous recombination predicts pathologic complete response to neoadjuvant chemotherapy in primary breast cancer. Clin Cancer Res 2010;16:6159–68.

36. Dumay A, Feugeas JP, Wittmer E, Lehmann-Che J, Bertheau P, Espie M, et al. Distinct tumor protein p53 mutants in breast cancer subgroups. Int J Cancer 2013;132:1227–31.

37. Drew Y, Mulligan EA, Vong WT, Thomas HD, Kahn S, Kyle S, et al. Therapeutic potential of poly(ADP-ribose) polymerase inhibitor AG014699 in human cancers with mutated or methylated BRCA1 or BRCA2. J Natl Cancer Inst 2011;103:334–46.

38. Turner N, Tutt A, Ashworth A. Hallmarks of 'BRCAness' in sporadic cancers. Nat Rev Cancer 2004;4:814–9.

39. Willers H, Taghian AG, Luo CM, Treszezamsky A, Sgroi DC, Powell SN. Utility of DNA repair protein foci for the detection of putative BRCA1 pathway defects in breast cancer biopsies. Mol Cancer Res 2009;7:1304–9.

40. Asakawa H, Koizumi H, Koike A, Takahashi M, Wu W, Iwase H, et al. Prediction of breast cancer sensitivity to neoadjuvant chemotherapy based on status of DNA damage repair proteins. Breast Cancer Res 2010;12:R17.

41. van Veelen LR, Cervelli T, van de Rakt MW, Theil AF, Essers J, Kanaar R. Analysis of ionizing radiation-induced foci of DNA damage repair proteins. Mutat Res 2005;574:22–33.

42. McGarry TJ, Kirschner MW. Geminin, an inhibitor of DNA replication, is degraded during mitosis. Cell 1998;93:1043–53.

43. Sundara Rajan S, Hanby AM, Horgan K, Thygesen HH, Speirs V. The potential utility of geminin as a predictive biomarker in breast cancer. Breast Cancer Res Treat 2014;143:91–8.

44. Gonzalez-Angulo AM, Timms KM, Liu S, Chen H, Litton JK, Potter J, et al. Incidence and outcome of BRCA mutations in unselected patients with triple receptor-negative breast cancer. Clin Cancer Res 2011;17:1082–9.

45. Hartman AR, Kaldate RR, Sailer LM, Painter L, Grier CE, Endsley RR, et al. Prevalence of BRCA mutations in an unselected population of triple-negative breast cancer. Cancer 2012;118:2787–95.

46. Mendes-Pereira AM, Martin SA, Brough R, McCarthy A, Taylor JR, Kim JS, et al. Synthetic lethal targeting of PTEN mutant cells with PARP inhibitors. EMBO Mol Med 2009;1:315–22.

47. Williamson CT, Muzik H, Turhan AG, Zamo A, O'Connor MJ, Bebb DG, et al. ATM deficiency sensitizes mantle cell lymphoma cells to poly (ADP-ribose) polymerase-1 inhibitors. Mol Cancer Ther 2010;9:347–57.

48. Bunting SF, Callen E, Wong N, Chen HT, Polato F, Gunn A, et al. 53BP1 inhibits homologous recombination in Brca1-deficient cells by blocking resection of DNA breaks. Cell 2010;141:243–54.

49. Edwards SL, Brough R, Lord CJ, Natrajan R, Vatcheva R, Levine DA, et al. Resistance to therapy caused by intragenic deletion in BRCA2. Nature 2008;451:1111–5.

50. Abkevich V, Timms KM, Hennessy BT, Potter J, Carey MS, Meyer LA, et al. Patterns of genomic loss of heterozygosity predict homologous recombination repair defects in epithelial ovarian cancer. Br J Cancer 2012;107:1776–82.

Clinical Cancer Research

Functional *Ex Vivo* Assay to Select Homologous Recombination–Deficient Breast Tumors for PARP Inhibitor Treatment

Kishan A.T. Naipal, Nicole S. Verkaik, Najim Ameziane, et al.

Updated version	Access the most recent version of this article at: doi:10.1158/1078-0432.CCR-14-0571
Supplementary Material	Access the most recent supplemental material at: http://clincancerres.aacrjournals.org/content/suppl/2014/06/28/1078-0432.CCR-14-0571.DC1

Cited articles	This article cites 50 articles, 9 of which you can access for free at: http://clincancerres.aacrjournals.org/content/20/18/4816.full#ref-list-1
Citing articles	This article has been cited by 10 HighWire-hosted articles. Access the articles at: http://clincancerres.aacrjournals.org/content/20/18/4816.full#related-urls

E-mail alerts	Sign up to receive free email-alerts related to this article or journal.
Reprints and Subscriptions	To order reprints of this article or to subscribe to the journal, contact the AACR Publications Department at pubs@aacr.org.
Permissions	To request permission to re-use all or part of this article, use this link http://clincancerres.aacrjournals.org/content/20/18/4816. Click on "Request Permissions" which will take you to the Copyright Clearance Center's (CCC) Rightslink site.